

NATIONAL ADVISORY COMMITTEE FOR AERONAUTICS

TECHNICAL MEMORANDUM 1380

CONTRIBUTION TO THE THEORY OF
TAIL-WHEEL SHIMMY

By M. Melzer

Translation of "Beitrag zur Theorie des Spornradflatterns." Bericht
der Focke-Wulf Flugzeugbau G.m.b.H., Bremen, Versuchsabteilung.
Technische Berichte, vol. 7, no. 2, 1940.

LIBRARY COPY



LANGLEY AERONAUTICAL LABORATORY
LIBRARY, NACA
LANGLEY FIELD, VIRGINIA

Washington

December 1954



CONTRIBUTION TO THE THEORY OF

TAIL-WHEEL SHIMMY*

By M. Melzer

The report shows, for simple cases, under what conditions tail-wheel shimmy - sometimes observed in rolling of airplanes - may occur. This is done by calculation of the stability limits decisive for rolling, with simplifying assumptions. The model tests are described which were performed for checking of the calculation results obtained and of the assumptions used.

OUTLINE

1. INTRODUCTION
2. THE STABILITY CONDITIONS FOR INFINITELY LARGE AIRPLANE MASS
3. INFLUENCE OF THE AIRPLANE MASS
4. CONCLUSIONS AND SUMMARY
5. REFERENCES

1. INTRODUCTION

In airplanes manufactured by various firms, oscillation phenomena on the tail wheels occurred in rolling and led to failures in some cases. One is dealing here with self-excited oscillations of the tail wheel and of the tail-wheel fork about the swivel axis of the latter, with the airframe participating in these oscillations to a higher or lesser degree according to the ratio of the masses and of the moments of inertia.

The tail-gear assembly should be constructed in such a manner that the swiveling part (that is, tail wheel plus tail-wheel fork) under the influence of the restoring forces assumes the mean position without oscillations

*"Beitrag zur Theorie des Spornradflatterns." Bericht der Focke-Wulf Flugzeugbau G.m.b.H., Bremen, Versuchsabteilung. Technische Berichte, vol. 7, no. 2, 1940, pp. 59-70.

when it had been deflected from the rolling direction by any force whatever (aperiodic stable motion). It is also still permissible that the swiveling part, after a deflection, passes several times through the zero position before it finally remains in the mean position (strongly damped oscillation). However, the rolling will be considerably disturbed when the damping of these oscillations becomes too small, zero, or worse, negative. In the last case the oscillations build up from, at first, small deflections to larger and larger ones until for some deflection a state of equilibrium is again established or failure of a structural member occurs.

The investigations described in the present report had the purpose of giving an explanation for the origination of these so-called shimmy oscillations and of demonstrating in general the influence of the various structural characteristics as far as this is possible in a method not applied to definite conditions. The numerical investigation required several assumptions and simplifications; in order to check their permissibility, a series of model tests were performed after the theoretical treatment, and were compared with the calculation.

2. STABILITY CONDITIONS FOR INFINITELY LARGE AIRPLANE MASS

For clarification of the question under what conditions tail-wheel shimmy occurs, the differential equations of motion were set up and Hurwitz' criteria of stability were used to examine under what conditions these equations have solutions with negative damping, that is, with self-excitation. As a result, one obtains one or more equations which indicate the boundary between stability and instability. They contain, in general, the conditions for static and dynamic stability; if a system is recognized as unstable on the basis of Hurwitz' stability criteria, periodic motions (tail-wheel shimmy) as well as aperiodic ones may occur.

In order to minimize nonessentials, the mass of the airplane was first assumed to be so large in comparison to the mass of the tail gear that the motion of the airplane is not influenced by the oscillations of the tail wheel. In the further course of the calculation, it will be indicated how the shimmy conditions vary when a motion of the airplane in one or several degrees of freedom is considered.

A number of forces act on the swiveling part which must be in equilibrium among themselves; the following symbols are used for the derivation of these equilibrium conditions (fig. 1):

- φ shimmy deflection
- ξ displacement of the center point of contact with respect to the wheel center plane, cm

a	distance of the wheel behind the swivel axis, cm
P	load on tail gear, kg
J_{ϕ}	moment of inertia of the swiveling part, referred to the swivel axis, cmkgs ²
$c_{r\phi}$	the springing coefficient of the wheel for forces acting perpendicular to the center plane at the point of contact, kg/cm
$c_{r\phi}$	the springing coefficient of the wheel for moments which twist the wheel around the perpendicular through the center point of contact, cmkg
$c_{F\phi}$	the springing coefficient of a tail-wheel restoring spring, cmkg
c_{ϕ}	the total springing coefficient opposing rotation of the wheel about the vertical ($c_{\phi} = c_{F\phi} + c_{r\phi}$), cmkg
ρ	the resistance coefficient for the rotation about the swivel axis, cmkgs
v	rolling velocity, cm/s
μ	friction coefficient between ground and wheel

The following moments act on the swiveling part, referred to the swivel axis:

1. The inertia resistance $-J_{\phi} \frac{d^2\phi}{dt^2}$.

2. The restoring moment $-c_{F\phi}\phi$. In the case of retractable tail wheels, there exists usually a spring which restores the tail gear to zero position. Even if one imparts to this spring (by catches and similar devices), a nonlinear regularity, it is, nevertheless, possible to indicate for small deflection angles, a constant springing coefficient $c_{F\phi}$.

A second restoring moment stems from the torsional elasticity of the tire; as long as the friction on the ground is sufficient, the tire attempts to restore again every rotation about the vertical, since it has contact with the runway not in a point but in a surface. The moment originating thereby has the value $-c_{c\phi}\phi$, so that, because of $c_{\phi} = c_{r\phi} + c_{F\phi}$, the total restoring moment becomes $-c_{\phi}\phi$.

3. All damping forces and moments which originate by bearing friction, material damping, and the like, are, in first approximation, put

proportional to the angular velocity of the swiveling part $\frac{d\phi}{dt}$. They are designated as the natural damping of the oscillation system. The sum of all these moments is assumed to be of the magnitude $-\rho \frac{d\phi}{dt}$.

4. Between runway and tire there originates a frictional force which acts at the point of contact at right angles to the wheel-center plane. Without discussing here its magnitude in detail, one may state that it laterally deforms the wheel. If one designates this deformation by ξ (fig. 1), and the springing coefficient of the wheel opposing this deformation by $c_r \xi$, the force is $c_r \xi$ and its moment about the swivel axis $ac_r \xi$.

The four moments named above must be in equilibrium at any instant. Therefore the equation

$$-J_\phi \frac{d^2\phi}{dt^2} - c_\phi \phi - \rho \frac{d\phi}{dt} + ac_r \xi = 0 \quad (1)$$

is valid.

Beside this equilibrium condition for the moments about the swivel axis, a second condition may be stated which asserts that the force $c_r \xi$ named in point 4 is balanced by the component S (lateral force) of the frictional force between runway and tire which is at right angles to the wheel center plane. The velocity and force relations on the rolling wheel can be seen from figure 2.

The airplane is rolling at the velocity v ; this velocity may be resolved into a velocity component in the wheel plane ($v \cos \phi$), and into a velocity component normal to the wheel plane ($v \sin \phi$). By rolling off the wheel would attain a peripheral velocity $v \cos \phi$ if no slip would exist between wheel and runway. Actually, however, the peripheral velocity is smaller (v_{RU}) since, due to the elastic deformation of the wheel, a sliding in the rolling direction occurs. Thereby, a slip of the rolling wheel is produced, of the magnitude

$$s = \frac{v \cos \phi - v_{RU}}{v \cos \phi} = \frac{\Delta v}{v \cos \phi} \quad (2)$$

The wheel point of contact has therefore a total velocity v_{BP} which is composed of Δv and $v \sin \phi$. The frictional force has the value μP with a direction opposed to the velocity v_{BP} so that the component S perpendicular to the wheel-center plane becomes

$$S = \mu P \cos \alpha \quad (3)$$

α may be expressed by φ and s

$$\tan \alpha = \frac{\Delta v}{v \sin \varphi} = \frac{s}{\tan \varphi} \quad (4)$$

If this value is introduced into equation (3), S becomes

$$S = \frac{\mu P}{\sqrt{1 + (s/\tan \varphi)^2}} \quad (5)$$

If one plots S against φ according to this equation, the following diagram results (fig. 3). For the wheel which is entirely free of slip ($s = 0$), the normal force increases immediately to its ultimate value μP for the deflection zero; for the wheel locked by brakes ($s = 1$), this force increases according to a sine law and attains the value μP for $\varphi = \pi/2$. The actual wheel lies, according to rigidity and friction, between these two lines; it must be noted that the slip s itself varies with φ so that the curve $S = f(\varphi)$ obtains a shape different from the form drawn. For the further investigation, the variation in the range of small deflection angles is important. The slope of the S/φ curve at the point $\varphi = 0$ is obtained from

$$\left. \frac{dS}{d\varphi} \right|_{\varphi \rightarrow 0} = \frac{\mu}{s} P \quad (6)$$

If one replaces the lowest part of the curve by a straight line, which can be done with very good approximation, one finds

$$S = \frac{\mu}{s} P \varphi = \mu' P \varphi \quad (7)$$

The friction value thus fixed at $\mu' = \mu/s$ must be determined from experiments for every wheel, every load, and rolling velocity since μ as well as s are dependent on these parameters.

If the swiveling part performs a rotation about the swivel axis with the angular velocity $d\varphi/dt$, there originates at the point of contact a lateral velocity $a d\varphi/dt$ (fig. 4); if, moreover, the wheel is deformed by ξ with the velocity $d\xi/dt$, the total velocity normal to the wheel plane becomes

$$v \sin \varphi + a \frac{d\varphi}{dt} + \frac{d\xi}{dt} = v \sin \varphi \pm a\varphi' + \xi' \quad (8)$$

The velocity of the point of contact varies thereby in magnitude and direction. The direction is given by

$$\tan \alpha = \frac{\Delta v}{v \sin \varphi + a\varphi' + \xi'} \quad (9)$$

and after introduction of s and φ

$$\tan \alpha = \frac{s}{\tan \varphi + \frac{a\varphi' + \xi'}{v \cos \varphi}} \quad (10)$$

As can be seen immediately from figure 4, the denominator of this expression equals $\tan \vartheta$, where ϑ is the angle between the velocity of the wheel center (v_{RM}) and the wheel center plane (sideslip or yaw angle). For transition to small angles, one finds for the case where a lateral motion of the point of contact is added to the rolling motion according to equation (7)

$$S = \frac{\mu}{s} P\vartheta = \mu' P\vartheta = \mu' P \left(\varphi + \frac{a}{v} \frac{d\varphi}{dt} + \frac{1}{v} \frac{d\xi}{dt} \right) \quad (11)$$

Since, as was mentioned before, the force S thus found must balance the elastic force $c_r \xi \xi$, the second condition of equilibrium becomes

$$c_r \xi \xi + \mu' P \left(\varphi + \frac{a}{v} \frac{d\varphi}{dt} + \frac{1}{v} \frac{d\xi}{dt} \right) = 0 \quad (12)$$

The two equations (1) and (12) represent the differential equations for the motion of the swiveling part and of the point of contact.

Without discussing in detail the complete solution of the equations of motion (1) and (12), one can determine, with the aid of Hurwitz' stability criteria, under what conditions the occurring oscillations are damped, undamped, or excited.

If one introduces the expressions

$$\varphi = \Phi e^{rt} \quad \text{and} \quad \xi = \Xi e^{rt} \quad (13)$$

wherein $r = d + i2\pi f$ (d . . . damping, f . . . frequency), into the equations named above and cancels out e^{rt} , one obtains from (1)

$$(-J_{\phi}r^2 - c_{\phi} - \rho r)\phi + ac_{r\xi}\Xi = 0 \tag{14}$$

from (12)

$$\left(c_{r\xi} + \frac{\mu'P}{v}r\right)\Xi + \mu'P\left(1 + \frac{a}{v}r\right)\phi = 0 \tag{15}$$

By elimination of ϕ and Ξ , there results from (14) and (15) the main equation of the system

$$\underbrace{J_{\phi} \frac{\mu'P}{v} r^3}_{A_0} + \underbrace{\left(J_{\phi}c_{r\xi} + \rho \frac{\mu'P}{v}\right)r^2}_{A_1} + \underbrace{\left(\frac{\mu'P}{v}c_{\phi} + \frac{\mu'P}{v}a^2c_{r\xi} + \rho c_{r\xi}\right)r}_{A_2} + \underbrace{\left(c_{\phi}c_{r\xi} + \mu'Pa c_{r\xi}\right)}_{A_3} = 0 \tag{16}$$

It can be shown that the system is stable under the conditions (and only under those conditions), that the coefficients A_0 to A_3 and the deter-

minant $D = \begin{vmatrix} A_2 & A_3 \\ A_0 & A_1 \end{vmatrix}$ are positive. Since the coefficients of the main

equation always are larger than zero, the stability of the oscillation diagram depends solely on the sign of the determinant. If one introduces into the latter the values for A_0 to A_3 , one obtains the following condition for stable rolling

$$\mu'P < ac_{r\xi} + \frac{\rho}{ac_{r\xi}} \left(\frac{\mu'P}{v} \frac{c_{\phi} + a^2c_{r\xi}}{J_{\phi}} + \frac{\rho c_{r\xi}}{J_{\phi}} + c_{r\xi} \frac{2v}{\mu'P} \right) \tag{17}$$

The frequency of the occurring oscillations may be given from the equation $(2\pi f)^2 = A_2/A_0$ as

$$f = \frac{1}{2\pi} \sqrt{\frac{c_{\phi} + a^2c_{r\xi} + \rho c_{r\xi}v/\mu'P}{J_{\phi}}} \tag{18}$$

The equation for the oscillation frequency applies rigorously only to the undamped oscillation; the self-excited as well as the damped oscillations more or less deviate in their frequency from the value thus calculated.

From equation (17), one recognizes that the rolling velocity v appears only in the expression which is dependent on ρ . If the natural damping of the oscillation system is small so that it may be neglected with respect to the other forces acting on the tail wheel, the conditional equation for stable running assumes the following extraordinarily simple form

$$\mu'P < ac_r\xi \quad (19)$$

Thus the wheel runs stably as long as the frictional force $\mu'P\phi$, produced by a deflection ϕ , is smaller than the deformation force $a\phi c_r\xi$, occurring from the same deflection.

If the complete equation (17) is solved with respect to ρ , ρ indicates a measure for the magnitude of the required damping if for structural reasons the rearward position resulting from equation (19) cannot be adhered to. This case is important particularly for nose wheels.

One recognizes from equation (17) that, in the case of swivel axis with high friction or with artificial damping, a stable region exists even for very small rearward positions since the second term on the right side of the equation then becomes larger due to $\rho/ac_r\xi$.

The influence of the rolling velocity will be expounded in more detail in the discussion of the test results.

Tests

As mentioned at the beginning, the results derived in the previous section were checked by means of model tests. For this purpose we used the test arrangement described below and represented in figure 5. Since it was important to make experiments also for the cases where the airplane mass can no longer be assumed as infinitely large or completely rigid, the arrangement of the test apparatus was already provided for these conditions; in particular, the rotation of the airplane fuselage about the longitudinal axis of the airplane had been taken into consideration.

The pipe 1 represents the mass of the fuselage; it may rotate about the longitudinal axis in a self-aligning ball bearing 2 and about this bearing as point of rotation in the perpendicular ($x - z$) plane. A motion out of this plane is prevented by the bearing-equipped guide 3. The rotation about the x axis is opposed by two springs 4. Adjustable masses 5 are rigidly connected to the pipe by which the moment of inertia about the longitudinal axis may be varied within broad limits. The

bearing load P of the tail wheel on the runway is adjusted by means of the sliding weight 6 and the spring 7. The tail wheel 8 consists of soft solid rubber; it is rotatable about the swivel axis 9; its distance behind the swivel axis a is adjustable. For the mounting of the swiveling part as well as of the tail wheel, ball bearings were used. In a few tests, a tail-wheel-restoring spring 10 was installed which restores the swiveling part to mean position in the range of small angles with linearly increasing moment. The tail wheel runs on a slightly roughened leather belt 11 which is driven by an electric motor.

Since for these first investigations the airplane mass was assumed to be so large that it was not influenced by the relatively quick motions of the tail gear, the rotation of the pipe 1 about the x axis had to be prevented. For this purpose the springs 4 were replaced by rigid connections and the swivel-axis bearing was laterally restrained.

The first measurements were to yield the initial values ($c_{r\xi}$, $c_{r\phi}$, $c_{r\psi}$, J_{ϕ} , μ') used in the equations (17) and (18). The springing coefficients of the wheel could be determined from the natural frequency of the swiveling part. With the belt stationery, the wheel was given a slight impact for various wheel-rear positions a and for several tail-wheel loads P , and the deflection curve was plotted. If one disregards the slight influence of the natural damping ρ , one obtains $4\pi^2 f^2 = (c_{\phi} + a^2 c_{r\xi}) / J_{\phi}$. If one plots therefore $4\pi^2 f^2 J_{\phi}$ against a^2 , a straight line must result which has a slope of $c_{r\xi}$ with respect to the abscissa and intersects the ordinate scale at the value c_{ϕ} . As an example, this curve has been plotted for the test series A2 in figure 6; since for this series a tail-wheel restoring spring had been installed, the oscillation frequency was measured once with this spring and once without it, and the springing coefficient $c_{r\psi}$ was determined from the difference.

In order to obtain the friction coefficients $\mu'P$, the deflection forces S were measured normal to the wheel plane for increasing deflection angles by means of a spring balance for all tail-wheel loads concerned; the rearward position of the wheel was selected as far to the rear as possible in order to avoid oscillations. The $\mu'P$ values were determined for various rolling velocities; however, the influence of the velocity was so small that it remained within the experimental scatter. The result of these measurements in the range of small angles (approximately up to 5°) is given in tables 3 and 4.

The moment of inertia of the swiveling part J_{ϕ} increases with increasing distance behind the swivel axis a . Its magnitude resulted from oscillation tests about the swivel axis set up horizontally for this purpose.

	a = 0.5	1	1.5	2	2.5	3	cm
$J\phi \times 10^2 =$	4.14	4.27	4.35	4.47	4.59	4.72	cmkgs ²

Shimmy tests. - In these tests the tail-wheel load P was adjusted, for a certain rearward position of the wheel a , in turn to $P = 1, 2, 2.8, \text{ and } 3.6$ kg by shifting of the weight δ and by compression of the spring 7 , and then the number rpm of revolutions of the driving shaft was regulated by stages between $n = 50$ and $n = 1000/\text{minute}$ corresponding to a velocity $v = 41.5$ and 830 cm/s. The range of revolution below $100/\text{minute}$ could not be satisfactorily evaluated because of uneven propulsion; the same was true for the range about $600/\text{minute}$ because of resonance between the natural frequency of the belt and the propulsion rotational frequency. At each rpm-stage the wheel was given a short impact; it was then observed whether oscillations of constant or of increasing amplitude occurred. If all decisive coefficients (for instance, for springing, friction, etc.) were constant - as they had to be assumed to be in the calculation - the amplitude of the occurring shimmy oscillation would increase more and more with time without attaining a fixed ultimate value. Actually, however, this is not the case; rather, the values are constant only in the range of small angles but vary with increasing deflection as was shown, for instance, for the value $\mu'P$ in figure 3. Hence, there appears in many cases a constant deflection which is the larger, the smaller the total damping of the system is under the various test conditions.

For a deflection of $\phi = \pm 45^\circ$, the swiveling part strikes against its limiting stops so that no larger deflections could be measured.

The tests were subdivided into two series, A1 and A2, which differ by the fact that for the tests of the first series no tail-wheel restoring spring was used whereas for the tests of the second series, a spring with a restoring moment of 19.7 cmkg had been installed. Due to changes on the wheel, the springing coefficients of the latter were, moreover, somewhat increased.

The numerical tables 1 and 2 contain the test results of both series: the deflections and frequencies measured for the various tail-wheel loads, rearward positions, and numbers of revolutions ($v_{\text{cm/s}} = 0.83n_{\text{min}^{-1}}$). As can be seen from the tables, the rearward position was changed each time by 0.5 cm; the limiting rearward position for which shimmying stops is, therefore, known, in general, only within this accuracy. When more exact data are given below, they have been derived from the variation of the deflections as a function of the rearward position.

The numerical tables 3 and 4 indicate the critical springing and friction coefficients for the two series. Furthermore, the result of the calculation is given as it was obtained from the equation (19) $a_{gr} = \mu'P/c_r\xi$. For comparison there appears underneath the limiting

rearward position a_{gr} from the test; this is that rearward position of the tail wheel for which, in the entire range of revolution (or velocity) investigated, no oscillations of constant or increasing amplitude occurred.

The comparison of test and calculation shows a satisfactory agreement so that one may regard as permissible the assumptions made for the investigation considered.

In the model test the rolling velocity did not play an essential role for answering the question whether or not shimmy is possible for certain tail-wheel loads, rearward positions, springing and friction coefficients. If one investigates the terms of the complete equation (17)

$$\frac{\rho}{ac_{r\xi}} \left(\frac{\mu'P}{v} \frac{c_{\phi} + a^2c_{r\xi}}{J_{\phi}} + \frac{\rho c_{r\xi}}{J_{\phi}} + c_{r\xi}^2 \frac{v}{\mu'P} \right) \quad (20)$$

which are dependent on the velocity and on the natural damping, one finds that they become infinitely large for $v = 0$ and $v = \infty$ so that for very small and for very large velocities, no shimmy oscillations are possible. In between a minimum value of the expression (20) lies at

$$v = \frac{\mu'P}{c_{r\xi}} \sqrt{\frac{c_{\phi} + a^2c_{r\xi}}{J_{\phi}}} \quad (21)$$

For checking of these relations in the model test, we plotted for a few tests the variation of the deflections for equal rearward position and equal tail-wheel load, but for different velocities, against the rpm of the shaft. As an example, we show this for the test of the series A2 with $P = 2.8$ kg and $a = 2.5$ cm (fig. 7). In this figure the value of the expression (20) is plotted neglecting the term $\rho c_{r\xi}/J_{\phi}$ for the values indicated in table 4, with consideration of the ratio between velocity and rpm of the driving shaft. ρ was inserted as 0.0186 cmkgs; since for $n = 770$ /minute the shimmy deflection becomes zero, the left side of the equation (17) is equal to the right one at this point, and one may calculate ρ from it. One sees from the comparison of this curve with the variation of 2ϕ from the test that the deflections 2ϕ are smallest in the range where the damping term is largest, and vice versa. Furthermore, one sees that the minimum value of the damping term lies at about $n = 140$ /minute with 0.52 kg so that the error of the simplified equation (19) amounts to only

$$\frac{0.52}{ac_{r\xi}} = \frac{0.52}{2.5 \times 4.25} 100 \text{ percent} = 4.9 \text{ percent}$$

One finds a further qualitative confirmation of equation (21) when considering tables 1 and 2. On the one hand, the rpm pertaining to the maximum deflection increases within the same series (A1 or A2) with increasing rearward position a and with increasing tail-wheel load P . On the other hand, these velocities lie, for otherwise approximately equal conditions, for the series A2 higher than for the series A1 as is to be expected on the basis of equation (21) from the difference of the c_{ϕ} values.

According to equation (17), it should be possible to find a stable range even for very small rearward positions since the second term of the right part of the equation then becomes very large. For satisfactory installation in the model test (small ρ) this stable position occurs for rearward offsets close to zero, and could therefore not be proved reliably.

3. INFLUENCE OF THE AIRPLANE MASS

Whereas, it was assumed in the investigations described so far that the airplane, due to its size, is not influenced in its motion by the tail-wheel oscillations, it will be indicated in the following section how the stability conditions vary if this simplifying assumption is dropped. We shall not attempt to give a complete solution for it since - with consideration of the numerous degrees of freedom of the motion of the airplane - the stability condition would contain so many parameters, and in very complicated relations, that a survey of the influence of the individual qualifying factors would not be possible after all. Conditions become more favorable only where one deals with the complete calculation of a definite case for which the majority of structural characteristics is fixed and only those need be considered which can still be modified by the type of construction of the tail-gear assembly.

In this part of the report we shall treat, as an example, the stability condition for the case that the airplane can rotate elastically about its longitudinal axis. Such a motion comes about when the airplane oscillates on the two front wheels due to alternating yielding of their tires. A similar motion occurs in the case of unsymmetrical forms of oscillation of the wing since here also the fuselage (and therewith the swivel axis) must perform torsional oscillations about the longitudinal axis (x axis) of the airplane.

For the numerical treatment of the degree of freedom of the motion thus fixed, the following symbols are used in addition to those enumerated in section 2 (fig. 8):

- λ deflection angle about the x axis (tramping angle)
- h distance of x axis from runway, cm

- J_λ moment of inertia of the airplane (or of the fuselage) about the x axis, cmkgs²
- J_{xz} centrifugal moment of swiveling part referred to the swivel axis and the x axis, cmkgs²
- J moment of inertia of tail wheel, referred to the tail-wheel axis, cmkgs²
- ω angular velocity of the tail wheel
- c_λ springing coefficient for the rotation about the x axis, cmkg

The equilibrium conditions of this oscillation form read:

1. Moments about the swivel axis (compare equation (1))

$$-J_\varphi \frac{d^2\varphi}{dt^2} - c_\varphi\varphi - \rho \frac{d\varphi}{dt} + ac_r\xi\xi - J_{xz} \frac{d^2\lambda}{dt^2} - J\omega \frac{d\lambda}{dt} = 0 \quad (22)$$

2. Moments about the x axis

$$-J_\lambda \frac{d^2\lambda}{dt^2} - c_\lambda\lambda - \rho_\lambda \frac{d\lambda}{dt} + hc_r\xi\xi - J_{xz} \frac{d^2\varphi}{dt^2} + J\omega \frac{d\varphi}{dt} = 0 \quad (23)$$

3. Equilibrium between frictional force and deformation force (compare equation (12))

$$c_r\xi\xi + \mu'P\left(\varphi + \frac{a}{v} \frac{d\varphi}{dt} + \frac{1}{v} \frac{d\xi}{dt} + \frac{h}{v} \frac{d\lambda}{dt}\right) = 0 \quad (24)$$

The following remarks are to be made regarding these equations:

To equation (22): The first four terms correspond exactly to equation (1). The fifth represents the mass coupling; if the swiveling part is deflected by λ , there originates at any arbitrary mass point of it an inertia resistance of the magnitude $-z \, dm \frac{d^2\lambda}{dt^2}$, if z is the distance of the point from the x axis. If one designates the distance from the swivel axis by x , the moment of this inertia resistance about the swivel axis becomes $-xz \, dm \frac{d^2\lambda}{dt^2}$, and for the entire swiveling part

$$-\int xz \, dm \frac{d^2\lambda}{dt^2} = -J_{xz} \frac{d^2\lambda}{dt^2} \quad (25)$$

The sixth term $-J\omega \frac{d\lambda}{dt}$ indicates the magnitude of the moment which is required for deflecting the tail wheel, rotating with the velocity ω , about the x axis with the angular velocity $\frac{d\lambda}{dt}$ (gyroscopic coupling).

To equation (23): This equation has a structure exactly corresponding to that of the previous equation, and expresses the equilibrium of the moments about the x axis.

To equation (24): The equation (11) states that the force component S of the frictional force μP , which is normal to the wheel plane, is proportional to the angle of sideslip ϑ . The angle of sideslip was given by the right part of the equation (11). Due to the motion of the swiveling part about the x axis, there originates at the point of contact of the wheel, a further velocity component of the amount $h \frac{d\lambda}{dt}$ so that the angle of sideslip becomes for this case:

$$\vartheta = \varphi + \frac{a}{v} \frac{d\varphi}{dt} + \frac{l}{v} \frac{d\xi}{dt} + \frac{h}{v} \frac{d\lambda}{dt} \quad (26)$$

For the further development, the terms $\rho \frac{d\varphi}{dt}$, $\rho\lambda \frac{d\lambda}{dt}$, $J\omega \frac{d\lambda}{dt}$, and $J\omega \frac{d\varphi}{dt}$ are neglected. Whereas the influence of the first two expressions can be estimated from the results of the first part, the influence of the gyroscopic coupling cannot be given immediately. One recognizes, however, that these terms also make the stability condition dependent on the velocity, and that this deviation must take effect for large velocities, since $J\omega$ vanishes for $v = 0$. It seemed useful to neglect the expressions mentioned above in the calculation, and to clarify the problem of the influence of the velocity by model tests carried out simultaneously.

For the determination of the stability condition, one uses again an expression of the form

$$\varphi = \Phi e^{rt}, \quad \xi = \Xi e^{rt}, \quad \lambda = \Lambda e^{rt} \quad (27)$$

If one introduces these expressions into the equations (22) to (24) and cancels out e^{rt} , there results three equations in r , Φ , Ξ , and Λ , the denominator determinant of which must disappear

$$\begin{vmatrix} -J_{\varphi}r^2 - c_{\varphi} & ; & -J_{xz}r^2 & ; & ac_r\xi \\ -J_{xz}r^2 & ; & -J_{\lambda}r^2 - c_{\lambda} & ; & hc_r\xi \\ \mu'P\left(1 + \frac{a}{v}r\right) & ; & \mu'P\frac{h}{v}r & ; & c_r\xi + \mu'P\frac{1}{v}r \end{vmatrix} = 0 \quad (28)$$

By solution of this determinant one obtains an equation of the 5th degree in r of the form

$$A_0 r^5 + A_1 r^4 + A_2 r^3 + A_3 r^2 + A_4 r + A_5 = 0 \quad (29)$$

with the coefficients

$$A_0 = (J_\varphi J_\lambda - J_{xz}^2) \mu' P/v$$

$$A_1 = (J_\varphi J_\lambda - J_{xz}^2) c r \xi$$

$$A_2 = (J_\varphi c_\lambda + J_\lambda c_\varphi + J_\varphi c r \xi h^2 + J_\lambda c r \xi a^2 - 2J_{xz} c r \xi a h) \mu' P/v$$

$$A_3 = (J_\varphi c_\lambda + J_\lambda c_\varphi + J_\lambda \mu' P a - J_{xz} \mu' P h) c r \xi$$

$$A_4 = (c_\varphi c_\lambda + c_\varphi c r \xi h^2 + c_\lambda c r \xi a^2) \mu' P/v$$

$$A_5 = (c_\varphi + \mu' P a) c_\lambda c r \xi$$

According to Hurwitz' investigations, the oscillation form is stable when A_1 , A_5 , and, in addition, the following determinants are larger than zero after A_0 has been made positive.

$$D_1 = \begin{vmatrix} A_2 & A_3 \\ A_0 & A_1 \end{vmatrix} \quad (30)$$

$$D_2 = \begin{vmatrix} A_3 & A_4 & A_5 \\ A_1 & A_2 & A_3 \\ 0 & A_0 & A_1 \end{vmatrix} \quad (31)$$

$$D_3 = \begin{vmatrix} A_4 & A_5 & 0 & 0 \\ A_2 & A_3 & A_4 & A_5 \\ A_0 & A_1 & A_2 & A_3 \\ 0 & 0 & A_0 & A_1 \end{vmatrix} \quad (32)$$

If even only one of these determinants becomes smaller than zero, self-excited oscillations or generally unstable motions of the system

occur. A survey of the stability conditions thereby obtained is considerably facilitated by the introduction of the following (dimensionless) quantities:

$$\alpha = \frac{c_{\phi}}{c_{r\xi} h^2} \quad \beta = \frac{c_{\lambda}}{c_{r\xi} h^2} \quad \gamma = \frac{\mu' P}{c_{r\xi} h} \quad (33)$$

$$\zeta = \frac{J_{xz}}{J_{\phi}} \quad x = \frac{J_{\phi}}{J_{\lambda}} \quad y = \frac{a}{h}$$

In order to obtain an idea of the influence of the individual parameters on the stability conditions, we performed initially a calculation for $\zeta = 0$. $\zeta = 0$ signifies that the swiveling part is statically and dynamically balanced with respect to the swivel axis, and that, therefore, the center of gravity of every section, laid parallel to the x axis, falls on the swivel axis. For the system simplified in this manner, the stability limits fixed by the determinants D_1 , D_2 , and D_3 become

$$\text{from } D_1 > 0: \quad x > y(\gamma - y) \quad (34)$$

$$\text{from } D_2 > 0: \quad \beta x^2 + \gamma y x > -y[\gamma y^2 + (\alpha - \gamma^2)y - \alpha y] \quad (35)$$

$$\text{from } D_3 > 0: \quad x[\beta y - (\beta + 1)\gamma] \leq [\gamma y^2 + (\alpha - \gamma^2)y - \alpha y] \quad (36)$$

for $x \leq \alpha/\beta$ and $y > 0$

If one represents the limits determined by (34) to (36) by $y = f(x)$, one obtains three limiting curves as plotted in figure 9. The numbers 1, 2, 3 assigned to the curves refer to the determinants D_1 , D_2 , and D_3 . Which one of the three curves indicates the actual limit depends on the ratio $\gamma^2/4 : \alpha/\beta$. Figure 9 is drawn for $\alpha/\beta > \gamma^2/4$. If, however, $\alpha/\beta < \gamma^2/4$, the lowest part of the limiting curve is modified according to figure 9a. The curve given by D_2 has not been plotted because it lies between 1 and 3 and is never the stability limit. The system appears stable when the first and third conditions are satisfied.

We shall point out in particular two characteristics of the limiting curves for the case $\zeta = 0$:

1. For $x = 0$, that is, for $J_{\phi} = 0$ or $J_{\lambda} = \infty$, one obtains $y = \gamma$; if one introduces again the original designations, this yields: $a/h = \mu' P / c_{r\xi} h$ or $a c_{r\xi} = \mu' P$, thus the condition found in section 2 (equation (19)) for the stability limit for the case of infinitely large airplane mass. This same limiting condition is valid with good approximation also for the points with small J_{ϕ}/J_{λ} as may be recognized from

the variation of the curve. One may also expect for this range that the dependence on the rolling velocity which is not contained in the equation due to the neglect of the natural damping is similar to the one derived previously.

2. The straight line $x = \alpha/\beta$ is a stability limit. With the original designations, the equation of this straight line is transformed into $\frac{J_\phi}{J_\lambda} = \frac{c_\phi}{c_\lambda}$ or $\frac{c_\phi}{J_\phi} = \frac{c_\lambda}{J_\lambda}$, that is, the system is stable only as long as the natural frequency of the swiveling part about the swivel axis (with the springing c_ϕ) is larger than the natural frequency of the airplane or of the airplane fuselage about the x axis. Closely below this limit (see fig. 9) the wheel runs evenly even for very small rearward positions whereas closely above it no stable run is attainable even for very large rearward positions.

Of particular interest is the question whether the lateral rigidity of the wheel $c_{r\xi}$ has in all cases such a decisive significance for the occurrence of tail-wheel shimmy as was found in the investigation of the case of infinite airplane mass (see equation (19)). Since the lateral rigidity of the wheel $c_{r\xi}$ is in the denominator of the values α , β , γ , all three expressions will become zero for the completely rigid wheel ($c_{r\xi} = \infty$). Only the ratios (α/β , β/γ) maintain their former values. The limiting curves thereby vary according to figure 10. For $x < \alpha/\beta = c_\phi/c_\lambda$ the system is always stable, whereas in the region $x > \alpha/\beta$, the stability range has increased and has been shifted into the range of smaller rearward positions. The horizontal asymptote decreases from $\frac{\beta + 1}{\beta} \gamma$ to $\gamma/\beta = \frac{\mu' P}{c_\lambda} h$.

The foregoing investigations of this section referred to the fully balanced swiveling part. If one eliminates this simplification, the stability conditions fixed by the determinants D_1 , D_2 , and D_3 , turn into the following equations:

$$\text{from } D_1 > 0: \quad x(1 + \gamma\xi - 2\xi y) > y(\gamma - y) \quad (37)$$

$$\begin{aligned} \text{from } D_2 > 0: \quad & (\beta x + \alpha + \gamma y - \gamma\xi x)(x + \gamma\xi x - 2\xi xy \\ & + y^2 - \gamma y) + (x - \xi^2 x^2)(\beta\gamma y - \alpha \\ & - \beta y^2) > 0 \end{aligned} \quad (38)$$

$$\begin{aligned} \text{from } D_3 > 0: \quad & (x + \gamma\xi x - 2\xi xy - \gamma y + y^2) [\alpha^2 + \alpha\gamma y \\ & + x(\beta^2 y^2 - \beta^2 \gamma y - \beta\gamma y + 2\alpha\beta\xi y \\ & + \beta\gamma\xi y^2 - \alpha\beta\gamma\xi - \alpha\gamma\xi)] - (x - \xi^2 x^2) \\ & \times (\beta\gamma y - \alpha - \beta y^2)^2 > 0 \end{aligned} \quad (39)$$

If one plots, in the same manner as for the mass-balanced swiveling part, y as a function of x , one obtains a variation similar to figure 9: figure 11. One notices as an essential difference that the rectangular set of straight lines (horizontal straight line from $x = 0$ to $x = \alpha/\beta$ and vertical straight line through $x = \alpha/\beta$) has become a curved line passing through the origin. In the range of small x values the branch of the limiting curve going through $x = 0$, $y = \gamma$ has not been changed greatly.

In the case of the balanced swiveling part, it has been pointed out that the natural frequency of the swiveling part c_ϕ/J_ϕ must be higher than that of the fuselage if stable rolling is to be attained without damping with wheel rearward positions equal to or smaller than $\mu'P/c_{r\xi}$. For the nonbalanced swiveling part one finds the corresponding condition by searching for the point of the limiting curve for which $y = \gamma$. If one substitutes $y = \gamma$ into the equation (39), one obtains after a few transformations

$$x = \frac{\alpha}{\beta} \frac{1}{1 + \zeta \left(\frac{\alpha}{\beta\gamma} - \gamma \right)} \quad (40)$$

Thus it is valid in first approximation for this case, too, that one must have $x < \alpha/\beta$, that is, $c_\phi/J_\phi > c_\lambda/J_\lambda$ if shimmy oscillations are to be prevented for relatively small rearward positions. Figure 12 shows the difference of the stability limits for a balanced swiveling part ($\zeta = 0$) for the following relationships

$$\begin{aligned} \alpha &= 0.0174 \\ \beta &= 1.2 \\ \gamma &= 0.115 \\ \zeta &= 0, \text{ respectively, } 2.25 \end{aligned}$$

Tests

Adjoining the calculation of the stability conditions, several model tests with the arrangement described in section 2 were carried out. They are to serve on the one hand for control of the calculation and its assumptions, and, on the other hand, are to show the influence of the rolling velocity which had dropped out of the stability equations due to neglect of the natural damping and the gyroscopic coupling. From the various test series which were performed for several tail-wheel loads and springing characteristics of the tail wheel and of the airplane fuselage about the x axis, two will be singled out here: One series with balanced swiveling part (series B7), and one with non-mass-balanced

swiveling part (series C1). For both series we plotted, on the basis of the stability conditions derived, the boundary $y = f(x)$ for values α , β , γ kept constant and then adjusted successively different rearward positions a of the tail wheel for a certain J_γ . Thereafter all rolling velocities in question were executed for every a ; every time the wheel was given a short impact, and the occurring oscillations were observed. The results are shown in the curves (figs. 13 and 14) by means of the type of designation of the test points. Points with equal moment of inertia J_λ have a common series symbol (for instance B71, B72, C11, C12, etc.). The characteristic values for the two series may be taken from tables 5 and 6.

The introduction of the value ζ - which had taken place already in the calculation - requires a certain explanation. ζ was determined by $\zeta = J_{xz}/J_\phi$. With increasingly rearward position of the wheel, J_{xz} increases; so does J_ϕ , but not in the same manner. Therefore, it cannot be expected that ζ remains equal for all rearward positions. And, it is not the case, either. Rather, ζ fluctuates for the test series C1 mentioned according to the following table 7.

The comparative calculation should be carried out for all these ζ values. This was omitted, however; we calculated throughout with $\zeta = 2.25$. We thus achieved numerically an essential simplification without significantly falsifying the result. The value 2.25 was singled out because it is a good mean value for the mean rearward positions which are of the greatest interest. On which side the error is made at the individual point may be estimated from consideration of figure 12, since here the curves for $\zeta = 0$ and $\zeta = 2.25$ are plotted.

Regarding the value $\zeta = 0$ of the series B7, it should be noted that it was realized in the test arrangement as closely as possible. The static equilibrium of the swiveling part about the swivel axis was achieved completely, the dynamic equilibrium, however, only with a more or less satisfactory approximation. Possibly this error could be the reason for the deviation between test and calculation in the region of the vertical stability limit at $x = 0.0232$.

In general, a comparison between test and calculation shows good agreement. Whereas, in the series B7, the influence of velocity is insignificant, it is found in series C1 in the sense that in the range of small x values, shimmy occurs particularly at small velocities and ceases in case of more rapid rolling, as known from the tests with infinitely large airplane mass. In contrast, the influence of the rolling velocity in the range of larger x values is exactly the opposite.

4. CONCLUSIONS AND SUMMARY

The conditions for a stable run of the tail wheel, that is, for the avoidance of shimmy oscillations were numerically investigated, under simplifying assumptions; the results obtained were checked by model tests. The essential assumption was that the center of gravity of the airplane moves rectilinearly in the rolling direction. The following degrees of freedom were treated:

1. Rotation of the swiveling part about the vertical swivel axis plus lateral deformation of the wheel, and
2. Rotation of the swiveling part about the swivel axis plus lateral deformation of the wheel plus rotation of the airplane, and therewith of the swivel axis, about the longitudinal axis of the airplane.

The complete calculation of the first case yielded as the most important result that the stable run of the tail wheel is dependent on a suitable rigidity of the wheel and, of course, also of its support in the lateral direction. In the case of practically frictionless mounting of the swivel axis, the equation (19): $\mu'P < ac_{r\xi}$ is decisive which states that the run of the tail wheel is stable as long as the frictional force (normal to the wheel plane) originating for a deflection φ is smaller than the deformation force $a\varphi c_{r\xi}$ appearing for the same deflection. For a given tail-wheel load, the stability is thus favorably influenced by a large distance of the wheel behind the swivel axis a , a large lateral rigidity of the wheel $c_{r\xi}$, and a small ground friction μ' . The rolling velocity has no effect on the onset of the shimmy oscillations. If, however, the mounting is affected by friction, or if dampers had to be applied for attainment of rolling stability, the stability conditions are regulated according to equation (17) which also shows the dependence on the rolling velocity.

For the second case where the rotation of the swivel axis about the longitudinal axis of the airplane was taken into consideration, the same distance of the wheel behind the swivel axis $a = \mu'P/c_{r\xi}$ is sufficient as long as the natural frequency of the swiveling part about the swivel axis - given by c_{φ}/J_{φ} - is sufficiently large with respect to the natural frequency of the airplane or the fuselage about the longitudinal axis of the airplane. This can be concluded from the behavior of the swiveling part possessing mass balance where for $c_{\varphi}/J_{\varphi} < c_{\lambda}/J_{\lambda}$ shimmy occurs for all distances of the wheel behind the swivel axis (fig. 9). For the nonbalanced swiveling part, the exact limit is fixed by the equation (40). If the ratio of the moments of inertia J_{φ}/J_{λ} is larger than the value determined by this equation, shimmy can be prevented only by very large distances of the wheel behind the swivel axis. Only when

the two natural frequencies lie sufficiently far apart, smaller distances of the wheel behind the swivel axis are again sufficient. In the range mentioned, tail-wheel shimmy may occur also for a perfectly rigid wheel (fig. 10), since the lateral elasticity of the wheel is replaced by the torsional elasticity of the fuselage (c_λ).

It appears expedient to determine, for the tail-wheel loads in question, the values μ' (for instance, on a concrete runway), $c_{r\xi}$ and therewith $a_{gr} = \mu'P/c_{r\xi}$ of the usual tail-wheel types by experiments since one must not select a distance behind the swivel axis smaller than a_{gr} if one wants to enforce a stable run without damping. The two quantities are the only qualifying parameters which must be known about the tail wheel to make the design of a stable assembly possible.

All considerations and tests were carried out with the swivel axis in vertical position. On the basis of the considerations which led to the determination of the stability conditions, it is immediately possible to draw conclusions as to the behavior in case of an inclination of the swivel axis, the more so, since for the usual tail-gear assemblies, only small angles of inclination have to be considered.

If one introduces into the differential and stability equations the normal distance of the point of contact from the swivel axis a (fig. 15) as the distance of the wheel behind the swivel axis, all equations remain valid, and it is clear that, for equal design of the tail gear, a will be the larger and the stability condition the more easily satisfied, the steeper the inclination of the swivel axis. It is true that the inclination of the swivel axis produces a restoring moment which is to be derived from the tail-wheel load and which should be included into the calculation of the amount of c_ϕ so that thereby the natural frequency about the swivel axis is increased. However, in the individual case, it must be examined whether it is not possible to produce the moment required for this purpose by a tail-wheel restoring spring of suitable dimensions, without reducing the distance a of the wheel behind the swivel axis.

A complete solution of the problem requires the consideration of all degrees of freedom of the motion of the airplane. As long as any motion of the overall center of gravity is disregarded, the following motions are of particular interest: the rotation of the airplane about the vertical axis, and the lifting motion of the swivel axis. This last mentioned motion originates through the deflection of the swiveling part about the inclined swivel axis.

The numerical treatment of these two additional degrees of freedom does not show any basic difficulties. A further differential equation would have to be set up for each one of them so that the denominator determinant becomes of the 7th or 9th degree. However, the solution of

the corresponding Hurwitz determinants results in a calculation expenditure which can be justified only in special cases.

Translated by Mary L. Mahler
National Advisory Committee
for Aeronautics

5. REFERENCES

1. Becker, G., Fromm, H., and Maruhn, H.: Schwingungen in Automobil-
lenkungen. Berlin: M. Krayn, 1931.
2. Hurwitz, A.: Mathematische Annalen, vol. 46 (1895), page 273.
3. Den Hartog, J. P.: Merchanische Schwingungen. Berlin: J. Springer,
1936.

TABLE I (Series A1)

n min-1	P = 1 kg		P = 2kg		P = 2.8 kg		P = 3.6 kg	
	2 θ °	f, cps						
a = 0.5 cm								
50	84	1.13	> 90	1.38	> 90	1.53	> 90	2.3
100	24	1.43	82	1.28	90	1.53	90	1.86
200	0	-----	70	1.33	90	1.42	90	1.58
300	↓		50	1.60	50	1.76	90	1.58
400			25	1.55	60	1.54	77	1.51
500			23	1.92	46	1.79	55	1.88
600			0	-----	0	-----	40	2.2
700							0	-----
800								
900								
1000								
a = 1 cm								
50	> 90	-----	> 90	-----	> 90	-----	> 90	-----
100	90	-----	90	-----	90	-----	90	-----
200	22	1.95	90	-----	90	-----	90	-----
300	0	-----	76	1.71	80	1.64	90	-----
400	↓		32	2.25	65	2.0	84	2.13
500			22	1.78	51	2.35	88	2.15
600			65	-----	64	2.23	75	2.22
700			0		22	2.73	54	2.66
800					36	2.6	34	2.74
900					0	-----	0	-----
1000								
a = 1.5 cm								
50	46	-----	> 90	-----	> 90	-----	> 90	-----
100	44	2	90	-----	90	-----	90	-----
200	30	2.35	70	2.25	90	-----	90	-----
300	0	-----	67	2.25	90	-----	90	-----
400	↓		22	2.55	84	2.6	87	2.7
500			82	2.2	61	2.7	78	2.8
600			54	2.55	60	2.8	80	2.2
700			0	-----	84	2.55	62	3.1
800					58	2.9	10	2.7
900					33	3.3	0	-----
1000					10	3.3		
1100					0	-----		
a = 2 cm								
50	27	-----	59	2.6	> 90	-----	> 90	-----
100	12	2.25	62	2.6	90	-----	90	-----
200	0	-----	78	2.7	90	-----	90	-----
300	↓		40	2.7	90	-----	90	-----
400			43	3.0	71	2.9	90	-----
500			24	2.7	60	3.0	90	2.9
600			20	2.55	40	3.3	66	3.15
700			0	-----	18	2.7	60	3.0
800					0	-----	15	4.1
900							0	-----
1000								
a = 2.5 cm								
50	0	-----	28	2.5	44	3.4	70	3.45
100	↓		30	2.7	59	3.46	90	3.20
200			30	3.16	82	3.02	90	3.2
300			18	3.25	76	3.3	90	3.3
400			17	3.46	42	3.45	80	3.25
500			0	-----	40	3.7	80	3.70
600					31	3.5	57	3.70
700					30	3.6	52	3.70
800					10	3.5	21	3.65
900					0	-----	10	4.10
1000							0	-----
a = 3 cm								
50	0	-----	0		10	3.95	20	4.30
100	↓				22	4.20	38	4.0
200					20	3.85	45	4.15
300					20	4.00	42	4.10
400					20	3.70	35	4.30
500					8	-----	20	4.40
600					0	-----	10	4.40
700							0	-----
800							0	-----
900							0	-----
1000								

a = 3.5 2 θ = 0 for P = 1 to 3.6 kg. } Beats

TABLE II (Series A2)

n min ⁻¹	P = 1 kg		P = 2 kg		P = 2.8 kg		P = 3.6 kg	
	2 ϕ^0	f, cps						
a = 2 cm								
50	0	----	27	4.6	45	4.65	60	4.6
100	↓		27	4.4	47	4.55	72	4.55
200			27	4.5	60	4.55	76	4.65
300			27	4.7	56	4.65	76	4.65
400			18	4.9	69	4.4	76	4.6
500			0		40	4.7	70	4.75
600			↓		27	5.1	46	5.1
700					30	5.1	44	5.1
800					27	5.2	40	5.25
900					21	5.45	25	5.5
1000	↓		↓		0		20	5.8
1100					↓		0	----
a = 2.5 cm								
50	0	----	0	---	20	5.5	21	5.45
100	↓		↓		27	5.45	38	5.3
200					30	5.5	41	5.35
300					29	5.5	51	5.4
400					26	5.65	47	5.35
500					22	5.6	40	5.4
600					15	5.9	21	5.75
700					0	----	10	6
800					0		20	5.85
900					↓		0	----
1000	↓		↓		↓		↓	
a = 3 cm								
50	0	----	0	---	0	----	0	----
100	↓		↓		↓		↓	
200								
300								
400								
500								
600								
700								
800								
900					↓		↓	
1000	↓		↓		20*	5.9	20*	6.0

*Belt resonance

TABLE III (Series A1)

P	kg	1	2	2.8	3.6
$\mu'P$	kg	7.83	10.65	12.3	13.1
$c_r\xi$	kg/cm	3.03	3.74	3.82	3.86
$c_\varphi = c_{r\varphi}$	cmkg	3.56	6.7	5.9	8.3
$a_{gr} = \mu'P/c_r\xi$	cm	2.58	2.85	3.22	3.40
From the tests a_{gr}	cm	2.5	3.0	3.1	3.4

TABLE IV (Series A2)

P	kg	1	2	2.8	3.6
$\mu'P$	kg	7.83	10.65	12.3	13.1
$c_r\xi$	kg/cm	4.0	4.1	4.25	4.5
$c_{r\varphi}$	cmkg	6	7	8	8
$c_\varphi = c_{r\varphi} + c_{F\varphi}$	cmkg	25.7	26.7	27.7	27.7
$a_{gr} = \mu'P/c_r$	cm	1.96	2.60	2.90	2.91
From the tests a_{gr}	cm	2.0	2 + 2.25	~2.7	~2.8

TABLE V - Moment of Inertia J_λ

For the series	B71 C11	B72 C12	B73 C13	B74 C14	B75 C15	C16	B76 C17
J_λ cmkgs ²	10.7	4.76	2.6	1.8	0.72	0.47	0.35

TABLE VI

Series	B7	C1
P kg	2.5	2.5
c_φ cmkg	54	33.6
c_λ cmkg	2320	2320
$c_{r\xi}$ kg/cm	4.2	4.2
$\mu'P$ kg	10.4	10.4
α	0.0278	0.0174
β	1.2	1.2
γ	0.115	0.115
ζ	0	2.25

TABLE VII

a cm	ζ
0	2.05
1	2.19
2	2.24
3	2.29
4	2.26
5	2.18
6	2.08
7	1.97
8	1.86
9	1.74

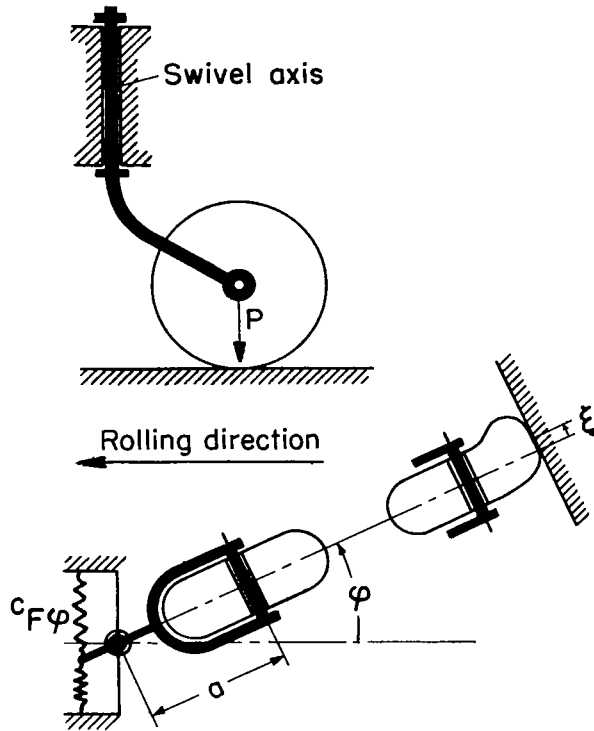


Figure 1.- Tail-wheel assembly.

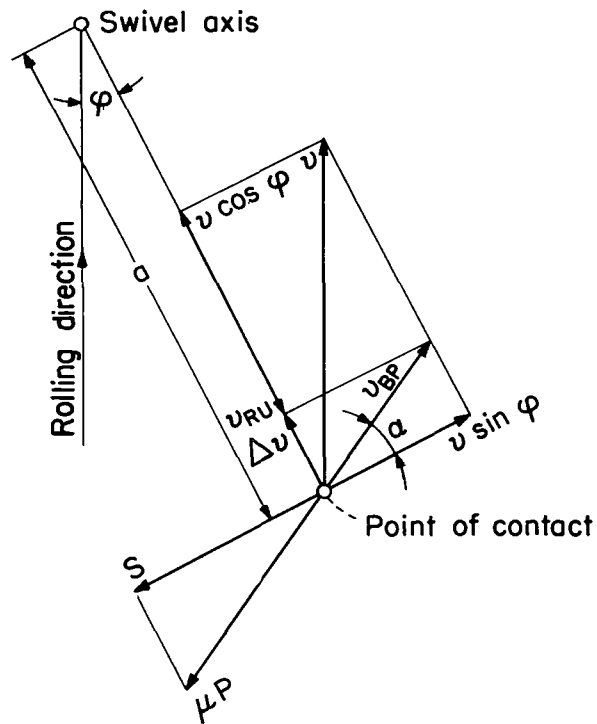


Figure 2.- Velocity and force relations for a deflected tail wheel.

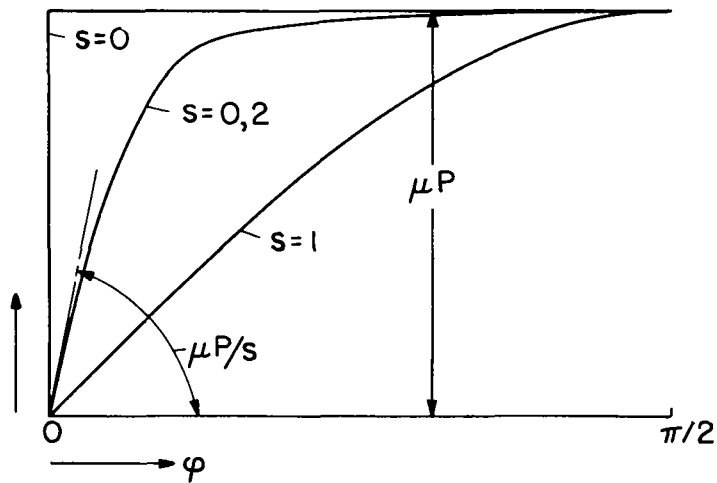


Figure 3.- Dependence of the lateral force S on the deflection angle.

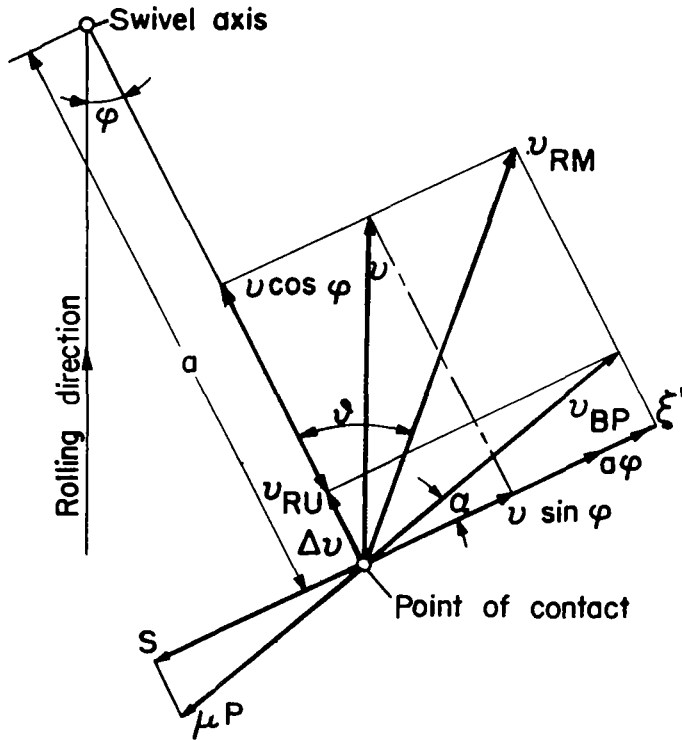


Figure 4.- Velocity and force relations for a deflected tail wheel for additional lateral velocity.

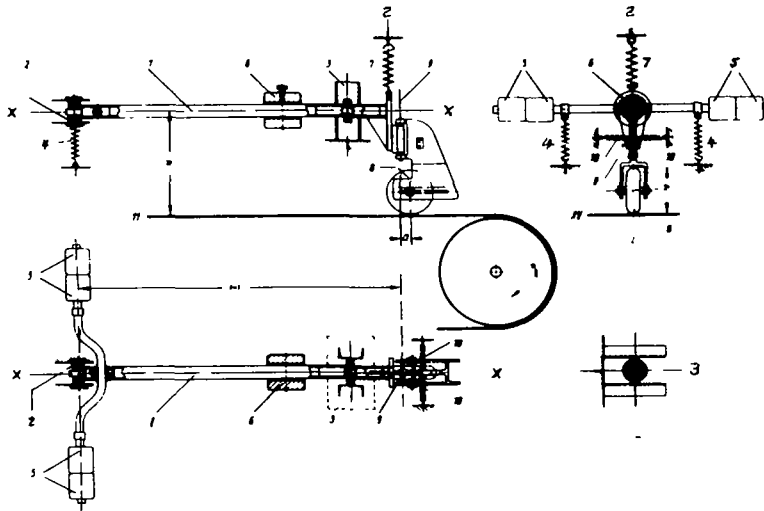


Figure 5.- Test setup.

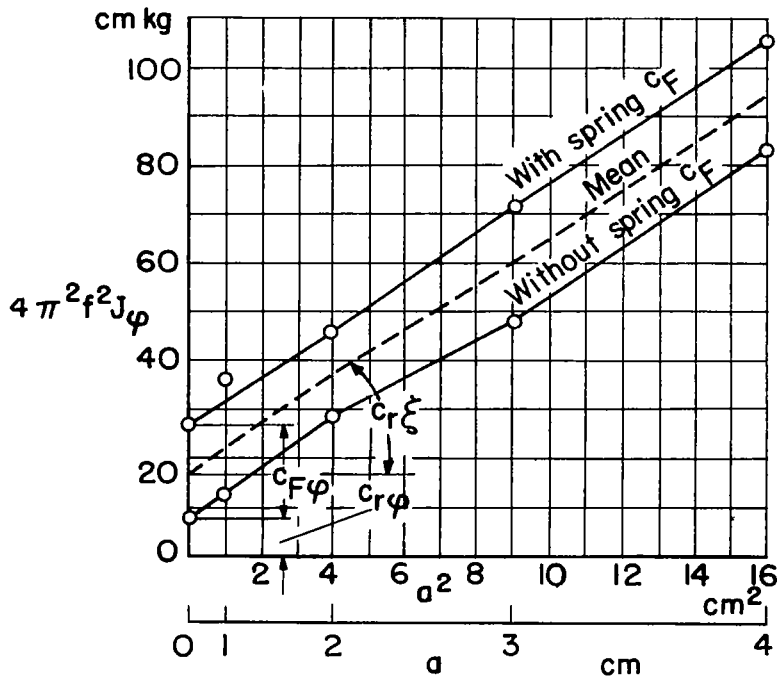


Figure 6.- Determination of the springing coefficients. $P = 2.8$ kg;
 $c_{r\xi} = 4.72$ kg/cm; $c_{r\phi} = 8$ cmkg; $c_{F\phi} = 19.7$ cmkg.

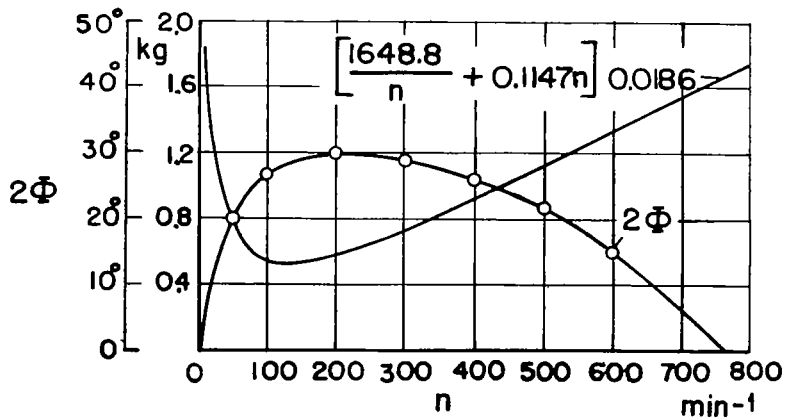


Figure 7.- Influence of the rolling velocity.

$$\frac{\rho}{ac_{r\xi}} \left(\frac{\mu' P}{v} \frac{c_\phi + a^2 c_{r\xi}}{J_\phi} + c_{r\xi} 2 \frac{v}{\mu' P} \right) = \left[\frac{1648.8}{n} + 0.1147n \right] 0.0186.$$

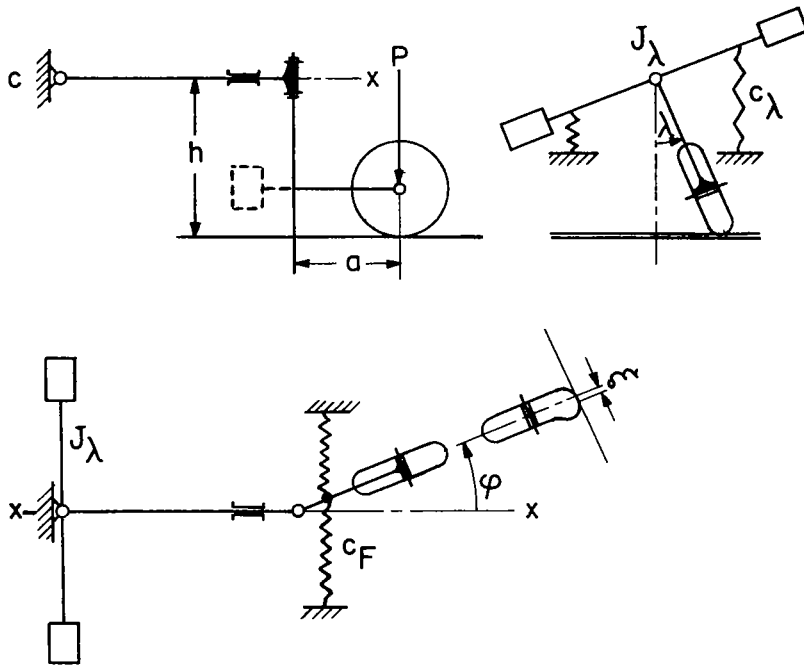
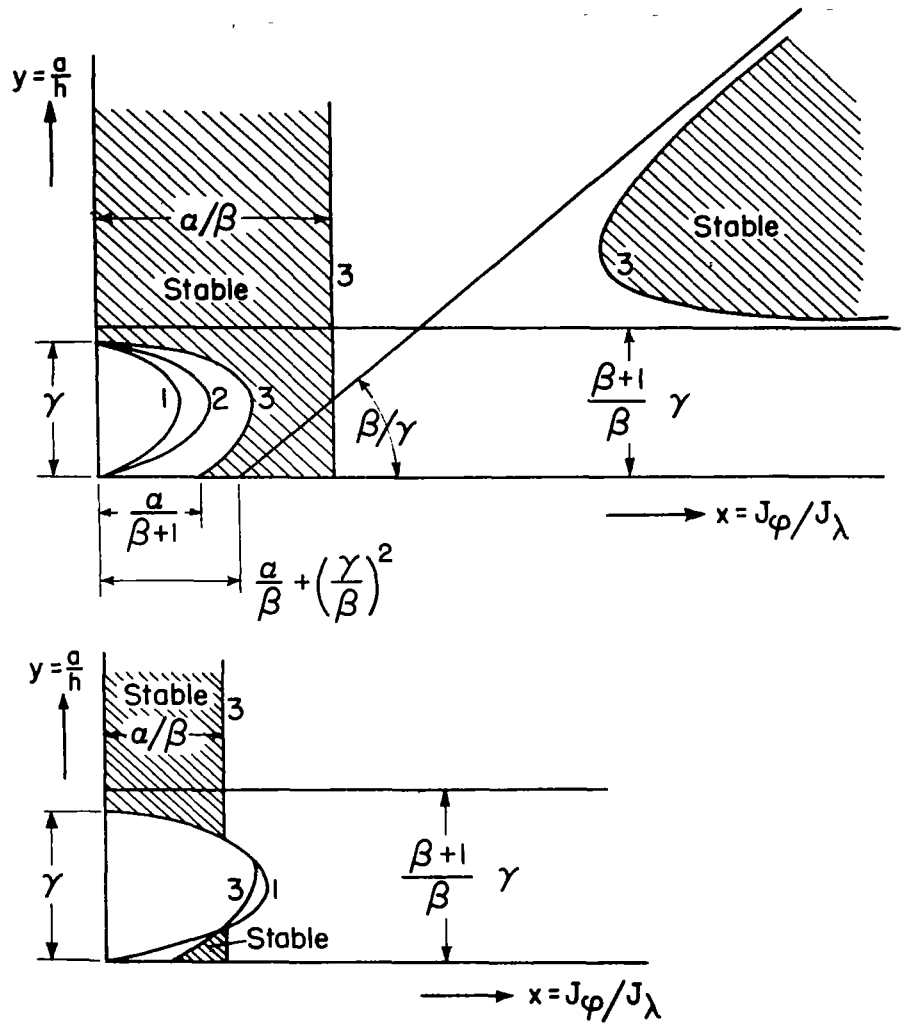


Figure 8.- Basic setup for rotation of the airplane about the x axis.



Figures 9 and 9a.- Stability conditions for a swiveling part possessing mass balance ($\xi = 0$).

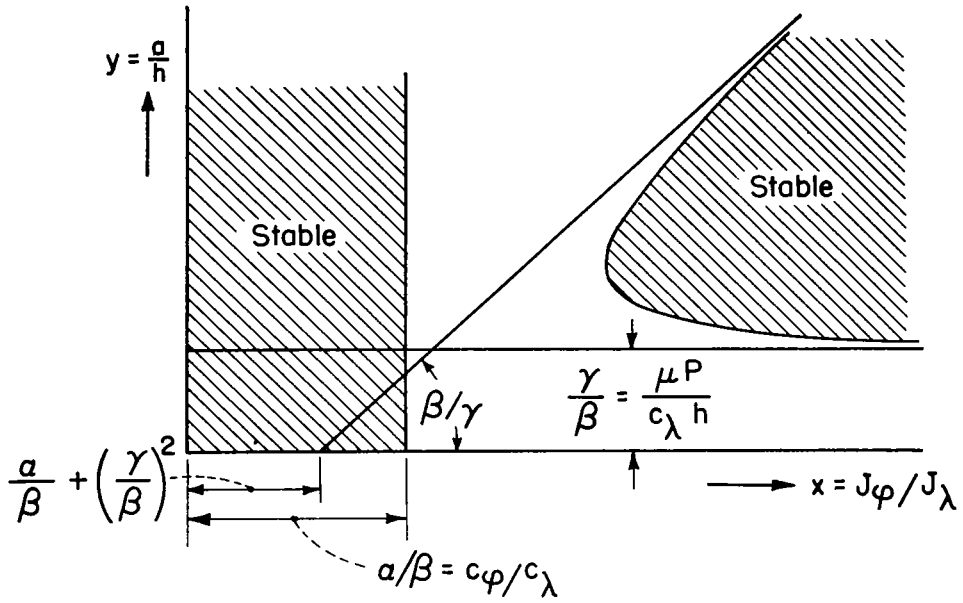


Figure 10.- Stability conditions for swiveling part possessing mass balance and perfectly rigid wheel ($c_{r\xi} = \infty$).

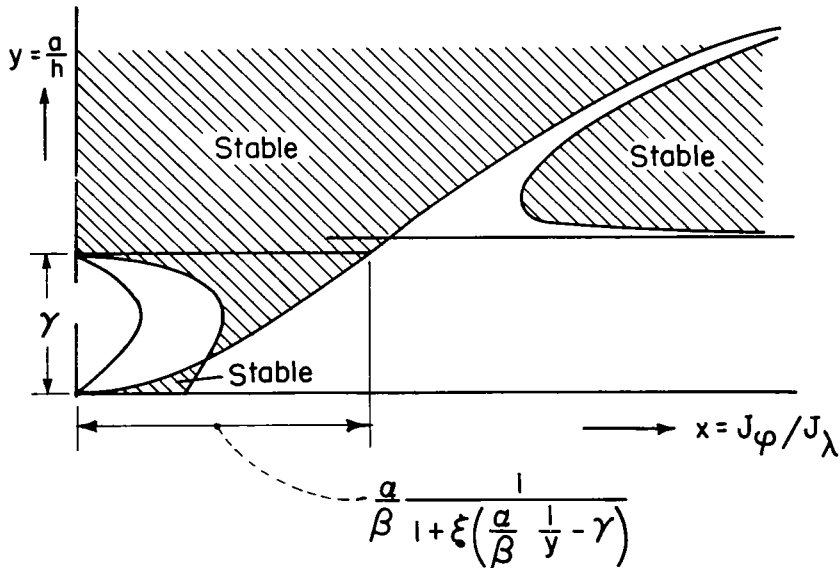


Figure 11.- Stability conditions for swiveling part not possessing mass balance ($\xi \neq 0$).

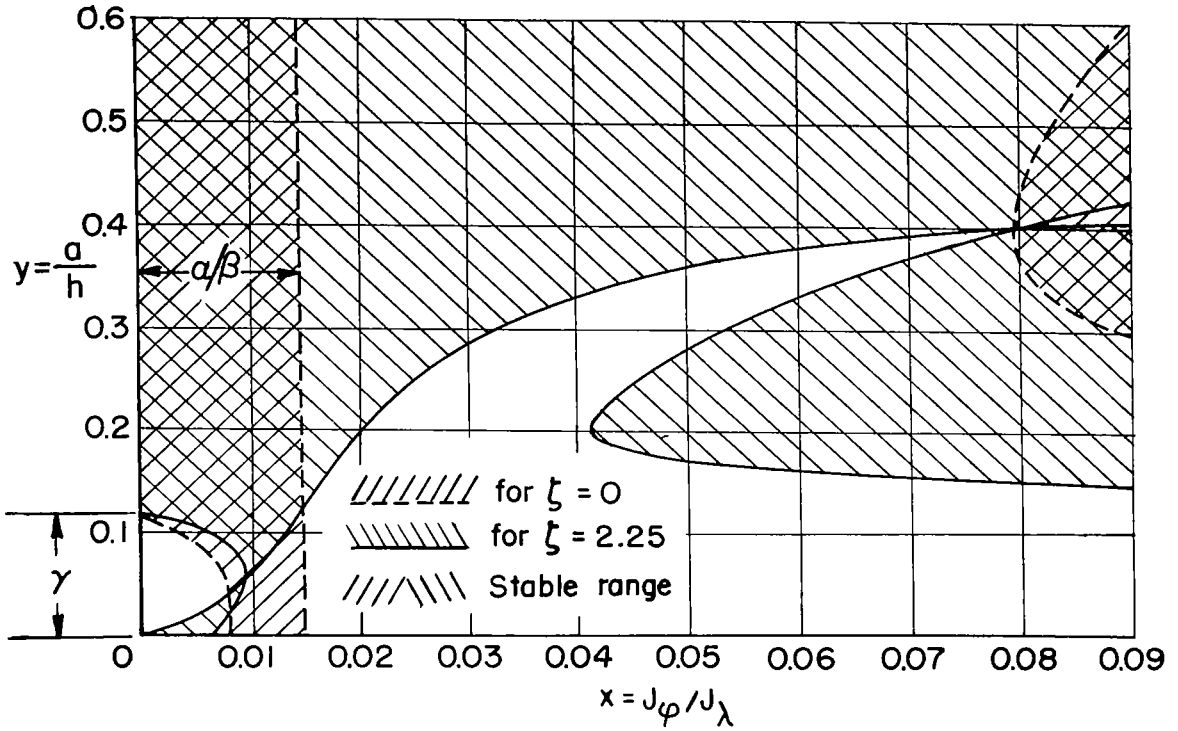


Figure 12.- Comparison between swiveling parts with and without mass balance.

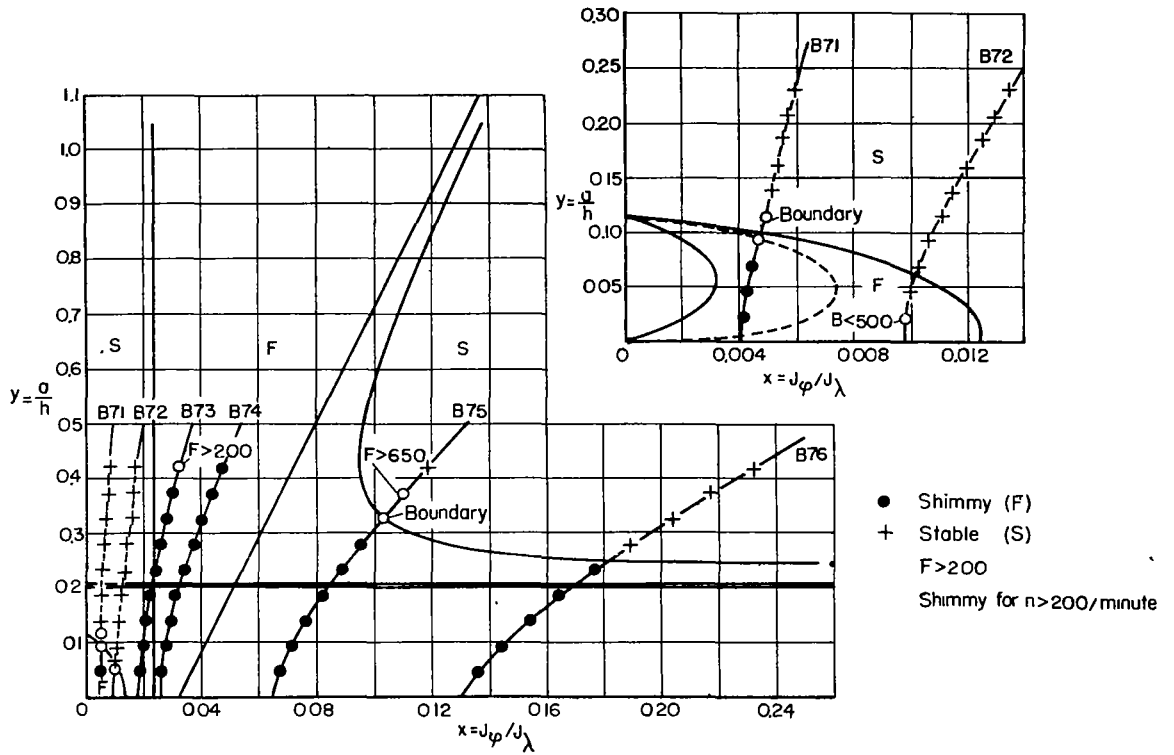


Figure 13.- Test B7; series B7. $P = 2.5$ kg; $c_{\phi} = 54$ cmkg; $c_{\lambda} = 2320$ cmkg; $\alpha = 0.0278$; $\beta = 1.2$; $\gamma = 0.115$.

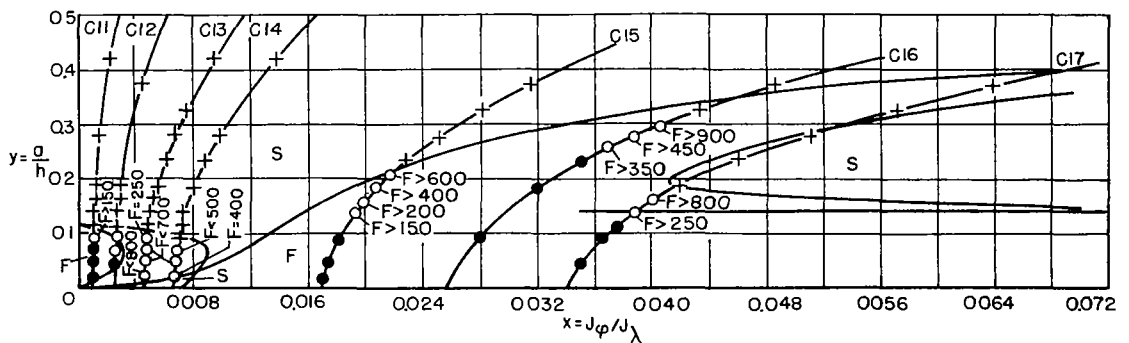


Figure 14.- Test C1; series C1. $P = 2.5$ kg; $c_{\phi} = 33.6$ cmkg; $c_{\lambda} = 2320$ cmkg; $\alpha = 0.0174$; $\beta = 1.2$; $\gamma = 0.115$; $\zeta = 2.25$.

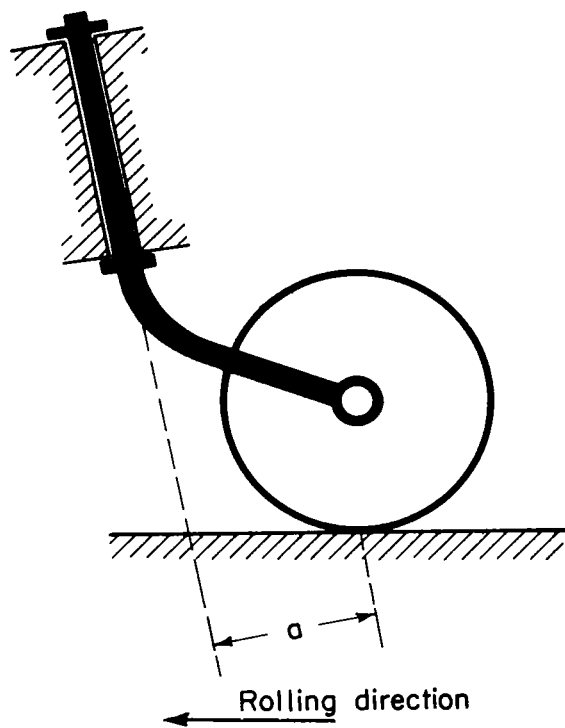


Figure 15.- Inclined position of the swivel axis.

NASA Technical Library



3 1176 01441 2119